

## Suppression of critical properties in doped cuprates

This article has been downloaded from IOPscience. Please scroll down to see the full text article.

2005 J. Phys. A: Math. Gen. 38 125

(<http://iopscience.iop.org/0305-4470/38/1/008>)

View [the table of contents for this issue](#), or go to the [journal homepage](#) for more

Download details:

IP Address: 171.66.16.66

The article was downloaded on 02/06/2010 at 20:02

Please note that [terms and conditions apply](#).

# Suppression of critical properties in doped cuprates

**E P Stoll**

Physics Institute, University of Zurich, CH-8057 Zurich, Switzerland

E-mail: [stoll@physik.unizh.ch](mailto:stoll@physik.unizh.ch)

Received 19 May 2004, in final form 28 October 2004

Published 8 December 2004

Online at [stacks.iop.org/JPhysA/38/125](http://stacks.iop.org/JPhysA/38/125)

## Abstract

In high- $T_c$  superconductors dopant atoms supply holes or excess electrons. Electric conduction happens in the neighbourhood of dopants within a circle several lattice constants wide. Percolation of these conducting areas leads to global conduction. Diffusing  $d$ -electrons in these areas can destroy antiferromagnetism: the Néel temperatures decrease with doping. Based on an Ising model with antiferromagnetic interactions acting in the part of the lattice not covered by conducting areas, the specific heat, the staggered susceptibility and the spin correlation lengths show very broad peaks even for low dopant concentrations. In doped cuprates, due to the small size granularity comparable with the sizes of our simulated systems, possible peak height singularities are always suppressed.

PACS numbers: 07.05.Tp, 64.60.Fr, 64.60.Ak, 75.30.Hx

## 1. Introduction

Most of the pure parent materials of high- $T_c$  superconductors are antiferromagnetic insulators. Susceptibility measurements show peaks at the Néel temperatures [1]. Electric conduction is established only by doping with, e.g., Sr in  $\text{La}_{2-x}\text{Sr}_x\text{CuO}_4$  (LASCO), oxygen in  $\text{YBa}_2\text{Cu}_3\text{O}_{6+y}$  (YBCO) or Ce in  $\text{Nd}_2\text{CuO}_4$ . The Néel temperatures decrease by doping and spin-glass-like states occur close to the magnetic percolation limit. Increasing doping transforms the system from an insulator into an electric conductor.

When some atoms are exchanged by others with a different valency, holes or excess electrons hop in regions delimited by a diameter  $d$  of several lattice constants  $a$ . By increasing doping conductive areas concatenate together to form percolating and conducting clusters [2–4]. The magnetic properties of these cuprates are very well understood [5], but there remain some open questions. To elucidate these properties a simple picture based on percolation and Ising antiferromagnetism has been used.

In two-dimensional  $N \times N$  spin lattices  $n$  different sites are chosen at random [6]. Each of these sites mark the origin of a circle with diameter  $d$ . If a new circle overlaps partially with

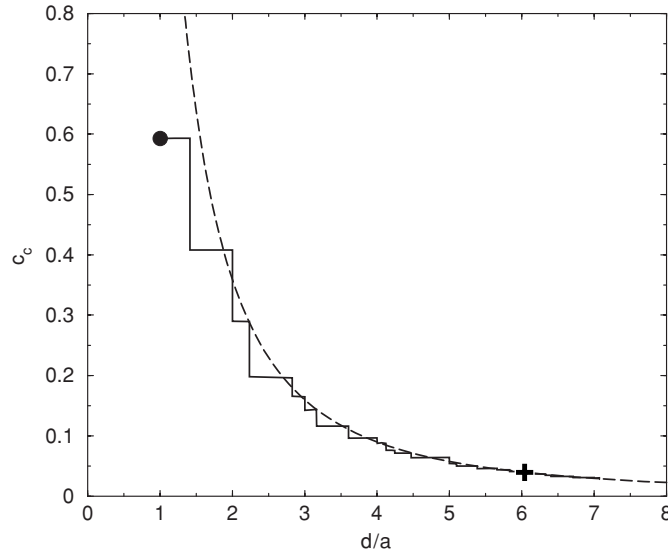


**Figure 1.**  $c_c = n_c/N^2$  as a function of  $d/a$ . The case  $d = a$  corresponds to site percolation on a square lattice. The full circle with  $c_c = p_c = 0.593$  is the theoretical value [11]. The dashed line is evaluated by  $\lim_{d \rightarrow 0} n(\Phi_c)d^2/[(aN)^2(d/a)^2] = -4/\pi \ln(1 - \Phi_c)/[(aN)^2(d/a)^2]$  for the cover  $\Phi_c = 0.6766$  of continuum percolation [13]. The cross at  $d/a \approx 6$  corresponds to the concentration  $c = 0.04 = x$  at the insulator–conductor limit of  $\text{La}_{2-x}\text{Sr}_x\text{CuO}_4$  [15].

older circles, they form a cluster. Cluster counting is accelerated by index registers [7, 8]. The total increase of the cover  $\Phi$  by the interposition of this new circle is made up of the sum of polygons and segments of the new circle and the subtraction of the areas of the segments of the older circles [9, 10]. All critical exponents  $\beta$  of the percolation order parameter are assumed identical to  $\beta = 5/36$ , the value for the two-dimensional site percolation problem [11]. Both  $(n_{pcl}/n)^7$  and  $(\Phi_{pcl}/\Phi)^7$  (the index  $pcl$  means belonging to the percolation cluster) are nearly linear functions of the circle concentration  $c = n/N^2$ , respectively  $\Phi$ , and can be fitted by straight lines. When these lines cross the value zero,  $\Phi_c$  or  $c_c$  are determined. In the case of continuum percolation [12], for which the lattice constant  $a$  tends to zero and  $Na$  remains finite, the critical cover  $\Phi_c = 0.677 \pm 0.001$  is in agreement with earlier results [13, 14].

For  $\text{La}_{2-x}\text{Sr}_x\text{CuO}_4$  the centres of the percolating discs correspond to the projection of the Sr atomic coordinates into the CuO plane. The net charge of the chemical unit cell after the La–Sr exchange is reduced by one. The occurring hole is attracted away from the position of the Sr atom by Coulomb forces. Because these forces are reduced by large dielectric constants, the diameters  $d$  of the circles in which the holes hop are limited to several lattice constants  $a$ .

## 2. Computer simulation results

We simulate the critical concentrations  $c_c = n_c/N^2$  as a function of  $d/a$  (the circle diameter  $d$  divided by the lattice constant  $a$ ) for  $d/a \geq 1$ . For  $d = a$  two neighbouring circles touch each other. As shown in figure 1,  $c_c$  corresponds to the percolation threshold  $p_c$  of site percolation on a square lattice [11]. By increasing  $d/a$ ,  $c_c$  remains constant until  $d/a$  reaches the value of  $\sqrt{2}$ , decreases by a jump and stays constant until the next jump. These abrupt changes for  $c_c$  occur when  $d$  correspond to the successive distance to the next neighbours and

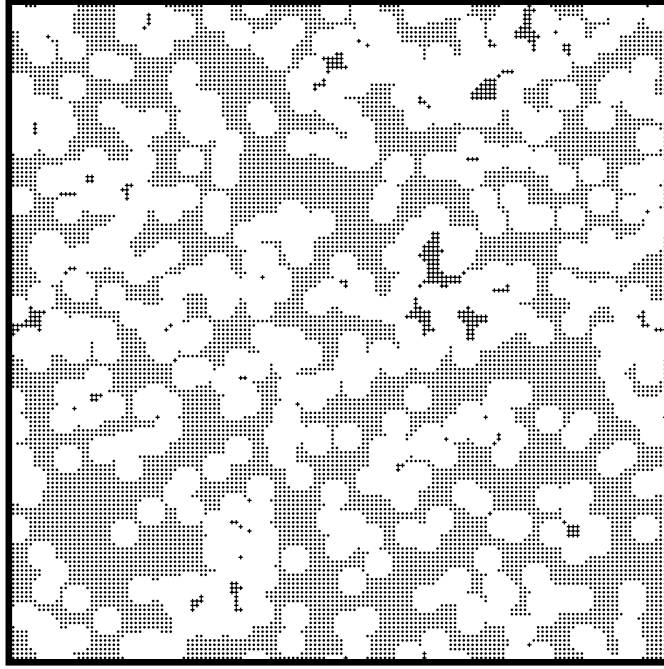


**Figure 2.** Snapshot of a  $151 \times 151$  sites antiferromagnetic lattice covered with 532 nonmagnetic spherical discs of a diameter  $d = 6.04$  lattice constants  $a$ . The concentration of disc centres is 0.023. The largest cluster, designated by points, contains 101 73 or 97% of all magnetic sites. All other cluster sites are designated by crosses.

resemble steps in a staircase. For large values of  $d/a$  and assuming that  $aN$  is a constant, namely one, this function can be approached by  $n(\Phi_c)d^2/[(aN)^2(d/a)^2] = \lim_{d \rightarrow 0} -4/\pi \ln(1 - \Phi_c)/[(aN)^2(d/a)^2]$ , where  $\Phi_c = 0.6766$  is the critical cover of continuum percolation [13].

In the structure of  $\text{La}_{2-x}\text{Sr}_x\text{CuO}_4$  the Sr atoms closest to the copper–oxygen plane are above or below this plane amid four copper atoms. The insulator–conductor transition occurs at a Sr atom concentration  $c = x \approx 0.04$  [15]. The cross in figure 1 for this  $c_c$  is placed at the centre of the constant step line with  $d/a = 6.04$ . The conducting discs cover an area of slightly more than  $6 \times 6$  lattice units. Holes or excess electrons hopping in the clusters are surrounded by diffusing  $d$ -electrons. Their spin direction is no longer localized on distinct places: antiferromagnetism breaks down. In  $\text{La}_2\text{CuO}_4$  the lattice of the La atoms is shifted against the Cu lattice by  $(a/2, a/2, \pm z_{La})$ . Therefore, the centres of the conducting circles are shifted against the underlying lattice by the same amount. A typical situation in a  $151 \times 151$  site spin-system is plotted in figure 2. The antiferromagnetic lattice (dots) is covered with 532 nonmagnetic white spherical discs of diameters  $d = 6.04$  lattice constants  $a$ . The concentration of disc centres is 0.023 and thus smaller than the critical concentration  $c_c = 0.028$  of the percolation limit of the spins. This small system is therefore percolating and illustrates clearly the characteristic connections between the spins. The conducting areas do not possess a perfect circular shape due to the coarse discretization.

To achieve reasonable statistics for determining the percolation threshold much larger systems ( $604 \times 604$  sites) have been investigated, and for each disc concentration  $c$  the percolation properties have been averaged over 500 different initial conditions. All chains

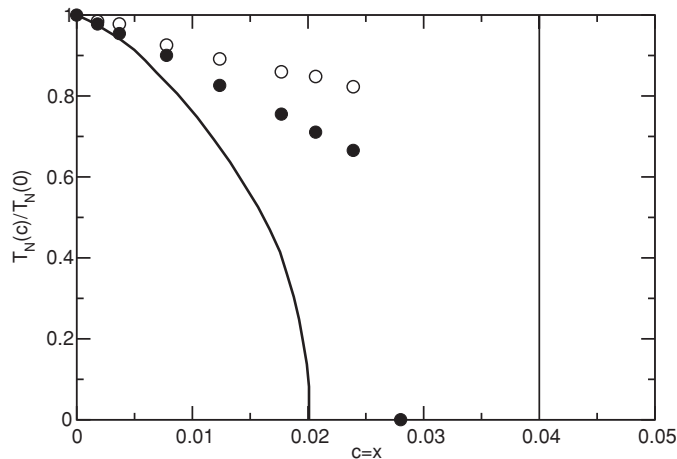


**Figure 3.** Néel temperatures of doped  $\text{La}_{2-x}\text{Sr}_x\text{CuO}_4$ . Solid line: experimental values [15]. Circles: Monte Carlo simulation of antiferromagnetic Ising system for  $d/a = 6.04$ . Full circles are calculated by extrapolations of the order parameter functions  $f(m(T))$  to zero. Open circles are determined using the  $T_m$  averages of the  $c_v$ ,  $\chi k_B T$  and  $\xi$ -peak maxima (figures 4, 5 and 6, definitions in the text). The vertical line at  $c = x = 0.04$  denotes the insulator–conductor transition.

of random numbers have been created by using a shift-register sequence random number generator [6]. They differ from each other for all new disc concentrations  $c$  as well as for all new temperatures  $T$  used by the Monte Carlo simulations. Because the critical disc concentrations  $c_c$  have shown dependences on  $d/(\text{Na})$ , simulations with  $d/(\text{Na}) = 0.01$ , 0.0142 and 0.02 are used for extrapolating  $c_c$  for  $d/(\text{Na}) = 0$ . The concentration  $c_c = x = 0.028$  of the doping Sr atoms in LASCO is smaller for percolation of the magnetic sites than the concentration  $c_c = x = 0.04$  for the insulator–conductor transition. This concentration is in agreement at least qualitatively (see figure 3) to the phase diagram of high- $T_c$  superconductors [15]. The reduction of  $T_N$  and the disappearance of the Néel states are due to the cut-off of magnetic interactions by nonmagnetic discs and not by vanishing percolation of magnetic regions as it was proposed [16] for explaining muon spin relaxation experiments.

We go back to the snapshot of a small system ( $151 \times 151$  sites) plotted in figure 2 with a disc concentration of 0.023. This is slightly less than 0.028 where antiferromagnetism vanishes, in order to present a stable percolation cluster. The distribution of discs and magnetic sites is rather inhomogeneous. There are large clusters of white discs enclosing magnetic sites being insulated from the percolation cluster. These insulated sites (plotted with small crosses) can change their Néel states faster and are not considered for the evaluation of the magnetic order parameter. They contribute, however, to spin glass properties. Due to the large inhomogeneities, Heisenberg systems of sizes large enough for reasonable statistics are very hard to simulate, and Ising spin systems have been used instead. The antiferromagnetic sites at the borders against the discs (see figure 2) have lost their interaction with one, two or three other sites. It becomes thus easier to reverse the spin directions by thermal fluctuations.

In order to obtain reasonable statistics on the values of thermodynamic properties, each property of one disc concentration and one temperature was averaged over 80 distributions of the nonmagnetic circles, generated with different random number chains [6]. The system size being used here was  $302 \times 302$  sites. Each new configuration started with all magnetic

spins pointing up. After an ageing time of  $n_a$  MC steps/spin all thermodynamic properties are averaged over  $n_a$  MC steps/spin. The smallest  $n_a$  used is 5000. Further  $n_a$  are chosen in steps so that they are twice the older ones until they reach 40 000. For temperatures close to the Néel temperature the specific heat and the susceptibility are evaluated by an extrapolation of  $n_a$  to  $\infty$  with  $\Delta 1/c_v$ ,  $\Delta 1/\chi$  and  $\Delta 1/\xi$  assumed proportional to  $1/n_a$ . The Néel temperatures are not easy to estimate due to finite size effects. In the infinitely large systems the coefficients  $\chi_0$  for the susceptibilities  $\chi$  with  $\chi = \chi_0(|(T - T_N)|/T_N)^{-\gamma}$  are much larger for  $T > T_N$  than for  $T < T_N$ . For finite systems the heights of the susceptibility peaks reach therefore their maxima at temperatures  $T_m > T_N$ . By identifying the Néel temperatures with  $T_m$  the critical exponents for the susceptibilities determined from log–log plots are different for  $T > T_N$  than for  $T < T_N$ . For infinitely large pure systems, all points of the function

$$f(m(T)) = 1 - \frac{\ln(\sqrt{2} + 1)}{\ln(1 + \{1 + [1 - m(T)^8]^{1/2}\}^{1/2}) - \frac{1}{4} \ln[1 - m(T)^8]}, \quad (1)$$

the inversion of Yang's [17] exact formula, lie on a straight line calculated with the order parameters  $m(T)$  of the pure two-dimensional Ising model. Applying equation (1) and fitting all points with not too small values by straight lines, the Néel temperatures  $T_N$  are determined as the intersection of these lines with the zero value [18]. It can be argued that this method may not be consistent with possible changes of the critical exponents [19, 20]. But other authors [18, 21–23] have shown that the critical exponents do not change so that this extrapolation is justified. It has been shown in the calculations for an earlier publication [18] that by determining  $T_N$  from equation (1) as explained above the critical exponents are the same for  $T > T_N$  and  $T < T_N$ . The Néel temperatures and the magnetic percolation limit are lowered for doped systems as plotted in figure 3. This figure shows furthermore that the extrapolations are closer to the experimental values [15] than  $T_m$ . The relative statistical uncertainties of  $T_N$  for low concentrations of nonmagnetic sites are of the order of 0.5% and close to the percolation limit of the order of 1.0%.

The specific heat functions  $c_v$  evaluated by considering energy fluctuations are plotted in figure 4. With increasing concentration  $c$  of dopant atoms very broad peaks appear. Their temperature dependences resemble theoretical results of systems with an infinite extension in one direction and finite free borders in the other direction [24]. This means that the free borders around the connecting discs act like the free borders in the theoretical calculations. Due to the close correspondence between the + signs, circles or triangles up (computations) and dashed, dash-dotted or dotted lines (theory [24]  $32 \times \infty$ ,  $16 \times \infty$  or  $8 \times \infty$ ) the average land-bridge width between the white clusters (as shown in figure 2) is in the order of 32, 16 or 8 lattice constants for a concentration  $c$  of 0.004, 0.007 or 0.014, respectively. The largest peak elevations for concentrations  $c$  close to  $c_c$  occur for temperatures larger than  $T_N$ . The Néel temperature is also shown for pure systems with finite sizes in figure 4 [25]. The large peak widths increasing with doping are traced back to the growing length of the free borders at the conducting circles, to the loss of translational invariance and to the random distribution of the dopants. Because cuprates are granular [26] there exist no such large size crystallites for which  $c_v$  may diverge. Furthermore, small grain sizes do not allow an unlimited growth of spectral densities. The peak broadening and the tiny peak heights presented in this figure persist therefore in doped cuprates.

A similar behaviour can also be observed in the isothermal staggered susceptibility diverging in a pure infinitely large system close to  $T_N$  with the critical exponent  $\gamma = 1.75$ . In figure 5 the theoretical curve is calculated according to [27]. Our results are evaluated using order parameter fluctuations. For an easy comparison for simulations of smaller and larger dopant concentrations the susceptibility is plotted on a logarithmic scale. As for the

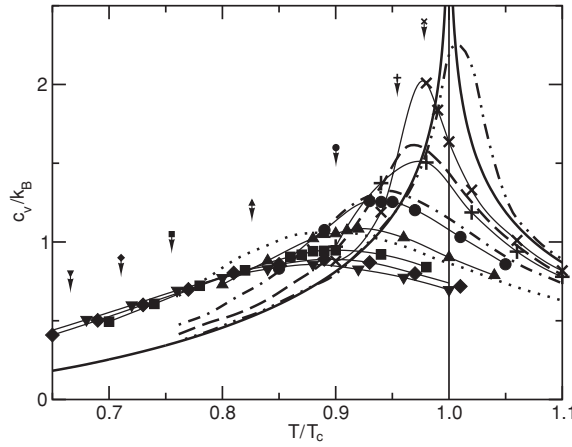


**Figure 4.** Calculated temperature dependence of the specific heat for a Sr concentration  $x = c$  of 0.001 79 (crosses), 0.003 67 (+ signs), 0.007 76 (circles), 0.0124 (triangles up), 0.0177 (squares), 0.0207 (diamonds) and 0.0239 (triangles down). The thin full lines are guide for the eyes. The relative uncertainties due to statistical fluctuations of the inhomogeneities and the Monte Carlo processes are of the order of 3% at each point. The remaining antiferromagnetic lattice has a size of  $302 \times 302$  sites (lattice constant  $a$ ), covered with nonmagnetic discs of diameter  $6.04a$ . Arrows denote the effective Néel temperatures. The thick full line corresponds to the exact specific heat of the pure system; the dashed, the dashed-dotted and the dotted line to a pure  $32 \times \infty$ ,  $16 \times \infty$  and an  $8 \times \infty$  lattice [24]. The dashed double-dotted line corresponds to calculations [25] of a system of  $64 \times 64$  sites.

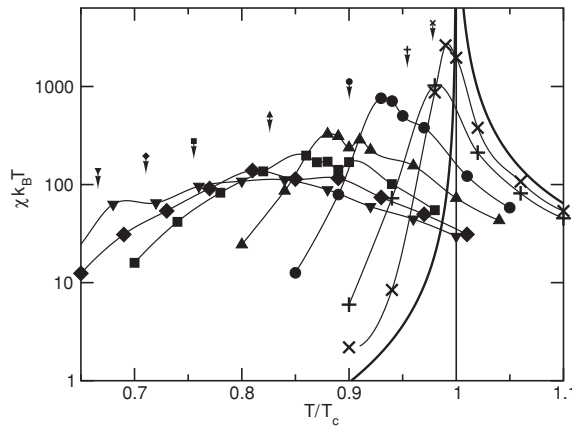


**Figure 5.** Calculated temperature dependence of the staggered susceptibility  $\chi k_B T$  for a Sr concentration  $x = c$  of 0.001 79 (crosses), 0.003 67 (+ signs), 0.007 76 (circles), 0.0124 (triangles up), 0.0177 (squares), 0.0207 (diamonds) and 0.0239 (triangles down). The thin full lines are guide for the eyes. The relative uncertainties due to statistical fluctuations of the inhomogeneities and the Monte Carlo processes are of the order of 6% at each point. The remaining antiferromagnetic lattice has a size of  $302 \times 302$  sites (lattice constant  $a$ ), covered with nonmagnetic discs of diameter  $6.04a$ . Arrows denote the effective Néel temperatures. The thick full line corresponds to the staggered susceptibility of an infinitely large pure system [27].

specific heat, a possible peak height increase is also stopped due to the small granular size of the cuprate grains.

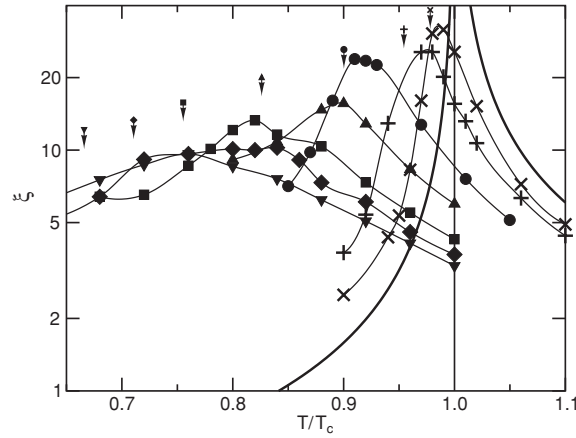


**Figure 6.** Calculated temperature dependence of the correlation parameter  $\xi$  for a Sr concentration  $x = c$  of 0.001 79 (crosses), 0.003 67 (+ signs), 0.007 76 (circles), 0.0124 (triangles up), 0.0177 (squares), 0.0207 (diamonds) and 0.0239 (triangles down). The thin full lines are guide for the eyes. The relative uncertainties due to statistical fluctuations of the inhomogeneities and the Monte Carlo processes are of the order of 10% at each point. The remaining antiferromagnetic lattice has a size of  $256 \times 256$  sites (lattice constant  $a$ ), covered with discs of diameter  $6.04a$ . Arrows denote the effective Néel temperatures. The thick full line corresponds to the  $\xi$  of an infinitely large pure system [27, 28].

A third critical property is the correlation length  $\xi(c, T)$ . In order to remove the problem of the oscillations in the two-point correlation functions due to antiferromagnetic ordering, their absolute values are considered.  $\xi(c, T)$  is determined by least-squares fits and by applying known pre-factor functions [27, 28]. The system size is reduced to  $256 \times 256$  sites for suitable applications of the fast Fourier transformations. For an easy comparison of differently doped slopes a logarithmic plot is used. Also here the peaks reach their maxima for slightly larger temperatures than the effective Néel temperatures (marked by arrows), and the peak widths become larger for higher impurity concentrations in agreement with the results for diluted magnets [20].

### 3. Summary and conclusions

It has been shown that in  $\text{La}_{2-x}\text{Sr}_x\text{CuO}_4$  high- $T_c$  superconductors the Néel temperatures decrease with increasing doping even when the systems are simulated with Ising instead of Heisenberg interactions. A system close to the magnetic percolation limit shows insulated small clusters responsible for the observed spin glass behaviour at low temperatures. The simulations of the specific heat show that the singularities of the infinite pure systems vanish for finite doped systems. Also, whereas it may not be excluded that for infinitely large doped systems the peak heights increase with system sizes, the small granular grain sizes of the cuprates [26] stop such an increase, so that the peak heights decrease and the peak widths grow with doping in those materials. A similar behaviour is also visible for the staggered susceptibility  $\chi$  and the correlation length  $\xi$ . Such a growth of the peak widths has also been observed in nuclear quadrupole resonance spectra of doped [29] superconducting  $\text{La}_{2-x}\text{Sr}_x\text{CuO}_4$  (LASCO), in contrast to the very narrow peaks of the pure antiferromagnetic isolator  $\text{La}_2\text{CuO}_4$  [30].



## Acknowledgments

We acknowledge fruitful discussions with T A Claxton, H Keller, M Mali, P F Meier, K A Müller, J Roos, T Schneider, D Stauffer and A-C Uldry.

## References

- [1] Johnston D C, Matsumoto T, Yamaguchi Y, Hidaka Y and Murakami T 1992 *Electronic Properties and Mechanisms of High  $T_c$  Superconductors* ed T Oguchi, K Kadowaki and T Sasaki (Amsterdam: Elsevier) p 301
- [2] Phillips J C 2002 *Phys. Rev. Lett.* **88** 216401
- [3] Phillips J C 2002 *J. Supercond.: Inc. Novel Magn.* **15** 393
- [4] Mihailovic D, Kabanov V V and Müller K A 2002 *Europhys. Lett.* **57** 254
- [5] Johnston D C *et al* 1997 *High- $T_c$  Superconductivity 1996: Ten Years after the Discovery* ed E Kaldis, E Liarokapis and K A Müller (Dordrecht: Kluwer) p 311
- [6] Kirkpatrick S and Stoll E P 1981 *J. Comput. Phys.* **40** 517
- [7] Hoshen J and Kopelman R 1983 *Phys. Rev. B* **28** 5323
- [8] Stoll E 1998 *Comput. Phys. Commun.* **109** 1
- [9] Stoll E P 2004 *J. Supercond.: Inc. Novel Magn.* **17** 79
- [10] Stoll E P 2004 *Int. J. Mod. Phys. C* **15** 321
- [11] Stauffer D and Aharony A 1994 *Introduction to Percolation Theory* (London: Taylor and Francis) revised 2nd edn
- [12] Domb C, Stoll E and Schneider T 1980 *Contemp. Phys.* **21** 577
- [13] Rosso M 1989 *J. Phys. A: Math. Gen.* **22** L131
- [14] Gawlinsky E T and Stanley H E 1981 *J. Phys. A: Math. Gen.* **14** L291
- [15] Poole Ch P, Datta T and Farach H A (ed) 1988 *Copper Oxide Superconductors* (New York: Wiley-Interscience)
- [16] Savici A T *et al* 2002 *Phys. Rev. B* **66** 014524
- [17] Yang C N 1952 *Phys. Rev.* **85** 808
- [18] Stoll E and Schneider T 1976 *J. Phys. A: Math. Gen.* **9** L67
- [19] Harris A Brooks 1974 *J. Phys. C: Solid State Phys.* **7** 1671
- [20] Stinchcombe R B 1983 *Phase Transitions and Critical Phenomena* vol 7 ed C Domb and J L Lebowitz (London: Academic) p 152
- [21] Domb C 1972 *J. Phys. C: Solid State Phys.* **5** 1399
- [22] Fisher M E and Au-Yang H 1975 *J. Phys. C: Solid State Phys.* **8** L418
- [23] Grinstein G and Luther A 1976 *Phys. Rev. B* **13** 1329
- [24] Au-Yang H and Fisher M E 1975 *Phys. Rev. B* **11** 3469
- [25] Ferdinand A E and Fisher M E 1969 *Phys. Rev.* **185** 832
- [26] Schneider T 2004 *J. Supercond.: Inc. Novel Magn.* **17** 41
- [27] Domb C and Green M S (ed) 1974 *Phase Transitions and Critical Phenomena* vol 3 (London: Academic)
- [28] Fisher M E and Burford R J 1967 *Phys. Rev.* **156** 583
- [29] Song Y-Q, Kennard M A, Lee M, Poppelmeier K R and Halperin W P 1991 *Phys. Rev. B* **44** 7159
- [30] Imai T, Slichter C P, Yoshimura K and Kosuge K 1993 *Phys. Rev. Lett.* **70** 1002